Homogeneous Conjugation of Peptides onto Gold Nanoparticles Enhances Macrophage Response

Neus G. Bastús,[†,▽] Ester Sánchez-Tilló,[‡,▽] Silvia Pujals,[§,▽] Consol Farrera,[‡] Carmen López,[⊥] Ernest Giralt,[§,¶] Antonio Celada,[‡] Jorge Lloberas,[‡,*] and Victor Puntes[†,#,*]

[†]Institut Català de Nanotecnologia, Campus UAB, 08193 Barcelona, Spain, [‡]Macrophage Biology Group, Institute for Research in Biomedicine, Barcelona Science Park and Department of Physiology, University of Barcelona, Barcelona, Spain, [§]Design Synthesis and Structure of Peptides and Proteins, Institute for Research in Biomedicine, Barcelona Science Park, Barcelona, Spain, [⊥]Unitat de Microscòpia Electrònica i Reconeixement Molecular *in Situ*, Serveis Científico-Tècnics, Universitat de Barcelona, [¶]Department of Organic Chemistry, University of Barcelona, Spain, and [#]Institut Català de Recerca i Estudis Avançats (ICREA) Barcelona, Spain. [▽]These authors contributed equally to this work.

Downloaded via EUROPEAN COMMISSION JRC on February 11, 2019 at 14:33:46 (UTC).
See https://pubs.acs.org/sharingguidelines for options on how to legitimately share published articles.

ABSTRACT Murine bone marrow macrophages were able to recognize gold nanoparticle peptide conjugates, while peptides or nanoparticles alone were not recognized. Consequently, in the presence of conjugates, macrophage proliferation was stopped and pro-inflammatory cytokines such as TNF-α, IL-1β, and IL-6, as well as nitric oxide synthase (NOS2) were induced. Furthermore, macrophage activation by gold nanoparticles conjugated to different peptides appeared to be rather independent of peptide length and polarity, but dependent on peptide pattern at the nanoparticle surface. Correspondingly, the biochemical type of response also depended on the type of conjugated peptide and could be correlated with the degree of ordering in the peptide coating. These findings help to illustrate the basic requirements involved in medical nanoparticle conjugate design to either activate the immune system or hide from it in order to reach their targets before being removed by phagocytes.

KEYWORDS: gold nanoparticles · peptide conjugation · immune system · proinflammatory response · cell internalization

The conjugation of inorganic nanoparticles to biological molecules, specially peptides and DNA, has created an expanding field of research that focuses upon the use of nanoparticle (NP) conjugates for diagnosis and therapy in biomedicine.[1] Despite the remarkable rapid development in strategies for particle conjugation, relatively little is known about NP behavior in complex biological systems. This is particularly true for the immune system, which is responsible for maintaining body integrity and preventing external invasion. Consequently, a profound understanding of the interaction between NPs and the immune system is needed if additional applications have to be developed.

Vertebrates are endowed with an immune system with two complementary branches, the innate and the adaptive, both of which must distinguish between self- and nonself molecules to protect the host from succumbing to infections. Phylogenetically ancient, the innate immune system provides the first line of defense against infections, typically triggering a protective inflammatory response within minutes.[2] If this proves insufficient in controlling the infection, the more highly sophisticated adaptive response is then induced. The key feature of innate immune cells enabling them to detect and categorize infection is their repertoire of pattern-recognition receptors (PRRs),[2] which bind certain types of molecules expressed by a broad class of pathogens. PRRs detect molecules known as pathogen-associated molecular patterns; however, this term is slightly misleading, as some of these molecules are not actually restricted to expression in pathogens.[3] In reality, what seems to distinguish a pathogen as nonself is the structural conformation of its molecules or their subcellular location.[3] This is consistent with detection of repetitive patterns in large structures such as in a virus capside.[4] Following these principles, it is of common knowledge that the artificial display of peptides, proteins, or antigens in an ordered, repetitive manner (epitope repetition), induces an enhanced immune response in comparison to vaccination with the "free" protein antigen.[5] In fact, lipoproteines/peptides (LP) are major constituents of the cell wall of bacteria and self-assembling proteins are the major constituents of virus capsides. In the case of natural pathogens, experiments indicate that the biological activity is more or less independent of peptide sequences in the LP library while the supramolecular conformation and the molecular shape are important features determining biological activity and the recognition

*Address correspondence to jlloberas@ub.edu, victor.puntes@icrea.es.

Received for review December 2, 2008 and accepted April 20, 2009.

Published online June 2, 2009.
10.1021/nn8008273 CCC: $40.75

© 2009 American Chemical Society

of patterns by TLR receptors,[6] a special family of PRRs.

In this paper we explore the ability of gold (Au) NP peptide conjugates to control the degree of immune system response. The main goals in this work are (i) to modulate the response of the immune system (vaccination, rejection, autoimmunity, allergies, and cancer) and (ii) to camouflage the conjugates from the immune system while trying to reach their target (when used as drug delivery vehicles or contrast agents for therapy or diagnosis). In this sense, previous results studying the interaction of NPs with human macrophages demonstrated that noncoated Au[7] and other NPs[7,8] did not elicit any strong immune response. However they seemed to bias naive macrophages and other cells of the immune system toward M1 polarized inflammation. As models for our work, two biomedically significant peptides were conjugated to Au NPs *via* the thiol of an N-terminal cysteine: (i) amyloid growth inhibitor peptide (AGIP) -CLPFFD-NH_2-, comprising amino acids 11 through 16 of the $A\beta_{1-42}$ protein, that recognizes a particular hydrophobic domain of the β-sheet structure and enables the selective attachment of Au NPs to β-amyloid fibers[9] (related to Alzheimer disease) and (ii) sweet arrow peptide (SAP) -$C(VRLPPP)_3$-, a nontoxic cell-penetrating peptide intended for intracellular drug delivery.[10] The chosen sequences are also known to have hydrophobic chains that promote their packing and aggregation. Their sequences are found in the core of dense aggregates as in the case of β-amyloid fibers and plaques. In addition, AGIP isomers (CLPDFF-NH_2 (ISO1) and CDLPFF-NH_2 (ISO2)), albumin fragments and serum (DMEM enriched with 10% of fetal bovine serum (FBS)) proteins were also conjugated to the Au NPs.

RESULTS AND DISCUSSION

Au NPs (10 nm) were synthesized based on the classical Turkevitch method (Figure 1, top). An 8 mg portion of hydrogen tetrachloroaurate was injected into a boiling 2.2 mM sodium citrate aqueous solution. We have observed that injecting the Au precursor into the hot reducing solution allows for a better size controlled system (monodispersity) than heating up the precursor solution before adding the citrate. All the peptides used in our studies present a thiol group on the side of the N-terminal cysteine (C) which makes a pseudocovalent bond (≈45 kcal/mol)[11] to the gold surface. The conjugation process was performed by incubating the Au NPs with an excess of (up to 100 times) the equivalent (10^{12} NP/mL; 0.2 nm^2 Au NP surface/peptide molecule,[12] leads to an initial 20 μM peptide concentration) of the peptide in an aqueous solution for 30 min to ensure rapid and full coverage. In such cases, when the peptide is linear, the terminal amino acid is highly hydrophilic and the core is more hydrophobic, water is excluded and a dense self-assembled monolayer is formed at the NP surface[13] leading to homogeneous conjugates. This was followed by 3 days of dialysis to remove the unbound peptide.

Citrate-stabilized Au NPs are stable in aqueous media and display the characteristic UV−vis absorption spectrum with a plasmon band at 518 nm. The absorption spectrum is sensitive to the NP environment and an observable red-shift of the surface plasmon resonance (SPR) band of about 8−10 nm appears once peptides are attached.[9] The shift occurs within a few minutes, suggesting that the conjugation process is quick. The spectra indicates that the solution are stable for weeks (Figure 1A). Simultaneously, the surface charge assessed by ζ-potential measurements confirms the conjugation process to be successful (Figure 1C). The ζ-potential value drops once peptides are conjugated. In detail, small variations are observed in the two conjugates: −7.3 mV in the case of AuNP-CLPFFD-NH_2 (AuNP−AGIP) which has one negative charge, and 2.3 mV in the case of AuNP-$C(VRLPPP)_3$ (AuNP−SAP), which has three positive charges in its sequence. The conjugation process was also followed by dynamic light scattering (DLS) where a clear increase in hydrodynamic size of the NPs (from 12.3 to 17.6 nm or 19.2 nm) is observed after conjugation (Figure 1E). Similarly, the conjugation of Au NPs to CLPDFF-NH_2 (ISO1) and CDLPFF-NH_2 (ISO2), which contain the same amino acids as CLPFFD albeit in a different sequence, was followed by UV−vis spectroscopy, DLS, and ζ-potential measurements (Figure 1B,D,F).

Further morphology and surface characterization was performed by high resolution TEM (HRTEM), electron energy loss spectroscopy (EELS) and X-ray photoelectron spectroscopy (XPS). XPS techniques were used to prove the presence of S−Au bonds on the surface (Figure 2). In the case of peptide-conjugated Au NPs, the expected peaks from S2p, S2s, and Au4f core levels were detected. The S2p signal consists of a broad band with a maximum at 168.2 eV corresponding to the chemisorption of sulfur grafted onto gold. This peak is a particularly good parameter since it is a singlet, thus making the interpretation straightforward. A similar trend (a broadening and a shift of the peaks) is also observed with the S2s photoelectron peak. In the case of capped Au NPs, part of the signal corresponding to Au 4f 7/2 shifts from 83.9 to 83.5 eV which relates to the Au−S surface bonds in a ratio that indicates full sulfidation of the surface.[9] The same result was obtained in alkanethiolates capped Au NPs.[14] High resolution TEM and EELS also showed the presence of the coating layer and the thiol binding molecule.[15] In the case of $C(VRLPPP)_3$ (SAP) conjugation, a low electronic density was observed around the Au NPs which suggests that the conjugation process adds 4 nm to the particle diameter. This is consistent with the bigger shift observed in the DLS measurements.

As conjugation of one peptide generates a homogeneous distribution of peptides on the Au NP surface,

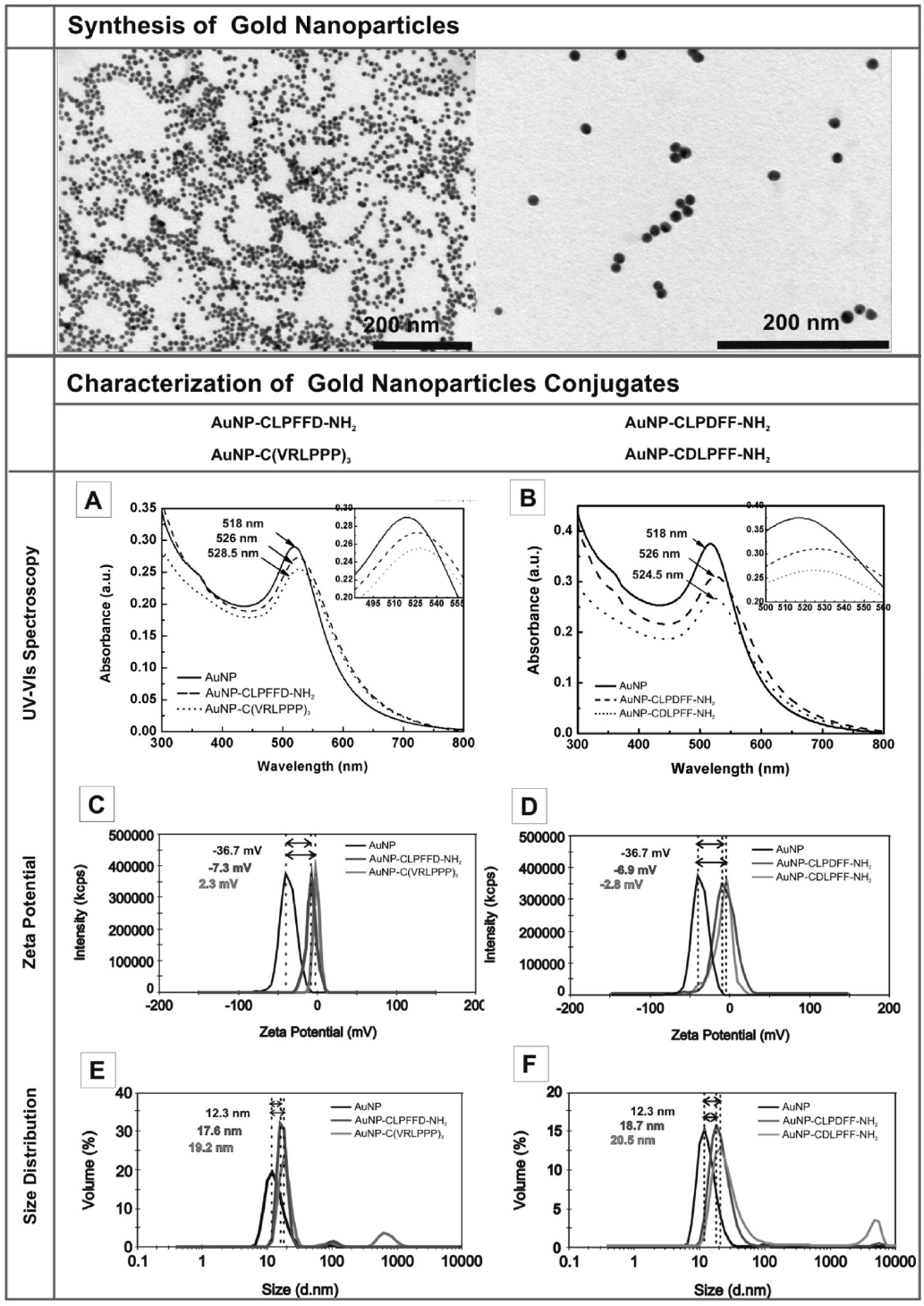

Figure 1. (Top) Gold nanoparticles. Transmission electron microscopy images of monodisperse citrate-stabilized 10 nm gold nanoparticles prepared by the sodium citrate reduction of hydrogen tetrachloroaurate. The colloid (10^{12} NP/mL) was drop-casted onto a Formvar carbon-coated copper grid for microscopy observation. The bar indicates 200 nm. (Bottom) UV−vis spectra, ζ- potential, and DLS characterization of peptide conjugated Au NPs. Characterization of conjugates AuNP-CLPFFD-NH_2 (AuNP−AGIP) and AuNP-C(VRLPPP)$_3$ (AuNP−SAP): (A) The red-shift in the position of the SPR band, (C) the drop of the Au NPs surface charge, and (E) the increase in the hydrodynamic radius confirm the conjugation process. Same results were obtained for AuNP-CLPDFF-NH_2 (AuNP−ISO1) and AuNP-CLPDFF-NH_2 (AuNP−ISO2) as can be seen in panels B, D, and F.

we also conjugated the Au NPs to a mixture of peptide sequences obtained from the reduced digest of bovine serum albumin (BSA) in order to obtain an heterogeneous peptidic coating. In detail, tris[2-carboxyethyl] phosphine (TCEP) reduced (to break disulfide bonds) BSA fragments (BSA_F), previously digested with trypsin, were conjugated to Au NPs. We used TCEP since it does not have thiols in its formulation, so it will neither attach to the Au NPs nor form disulfide bonds with peptides. BSA degraded by trypsin results in 78 different

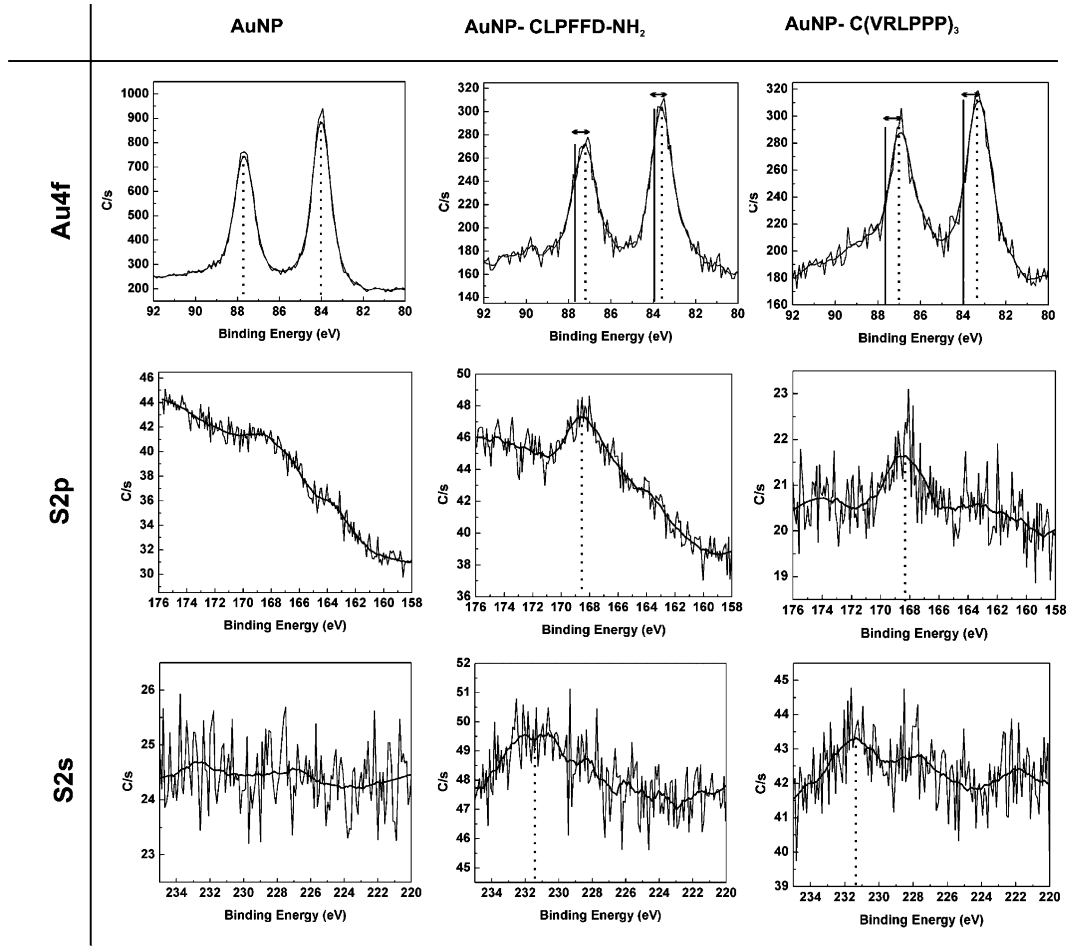

Figure 2. High-resolution XPS spectra of AuNPs, AuNP-CLPFFD-NH2 (AuNP−AGIP), and AuNP-C(VRLPPP)$_3$ (AuNP−SAP): (top) Au 4f region, (middle) S2p region, and (bottom) S2s region.

peptide sequences, 24 of them containing a cysteine, and thus being able to strongly attach to the Au NPs. In these experiments, full coverage of the Au NPs was again followed by the red-shift in the SPR band (from 518 to 522 nm), surface charge (from −38.9 to −19.6 mV) and DLS (from 12.8 to 18.2 nm).

We also note that when NPs are exposed to biological media, proteins, peptides, and amino acids compete for the NPs surface leading to a nonspecific conjugation. Therefore, we carried out different experiments exposing Au NPs to cell culture media (DMEM, without phenol red, + 10% FBS) and monitoring the nonspecific (and heterogeneous) NP coating by UV−vis, surface charge, and DLS. As expected, the red-shift in the SPR peak (518 to 526 nm), as well as the drop in surface charge (−38.9 to −21.2 mV) and the increase in the hydrodynamic size (from 12.8 to 17.1 nm) indicated the conjugation of Au NPs to sulfide- or disulfide- (preferentially) containing proteins, peptides, and amino acids present in the cell medium.

We also performed the citrate-stabilized Au NPs and conjugates in an agarose gel electrophoresis in phosphate buffer at pH 7.0 (see Supporting Information). Electrophoresis is sensitive to the size and surface charge of Au NPs and conjugates.[16] Citrate-stabilized Au NP particles did not migrate in the running conditions (they tend to aggregate due to the high medium salinity) while conjugates migrated either in a narrow band, when they bore a homogeneous coating (AuNP-CLPFFD-NH$_2$, AuNP-CLPDFF-NH$_2$, AuNP-CDLPFF-NH$_2$, AuNP-C(VRLPPP)$_3$) or in a broad band, when they bore a heterogeneous coating (Au NPs conjugated to BSA fragments or serum proteins). In the case of different sequences, small variations were observed and they were attributed to the fact that the more packed the monolayer is, the better the conjugate travels through the gel.[17] Conjugates were stable in the cell culture media through all of the experiments.

To test whether and how Au NPs and their conjugates activate the immune system, mouse bone marrow macrophages, obtained from BALB/c mice, were used as *in vitro* cell models for a primary culture of macrophages.[18] Macrophage proliferation is a well established method to verify macrophages activation since *in vitro* exposition of macrophages to pathogens and microbial substances blocks proliferation and promotes the acquisition of effector functions.[19,20] This includes the production of pro-inflammatory cytokines,

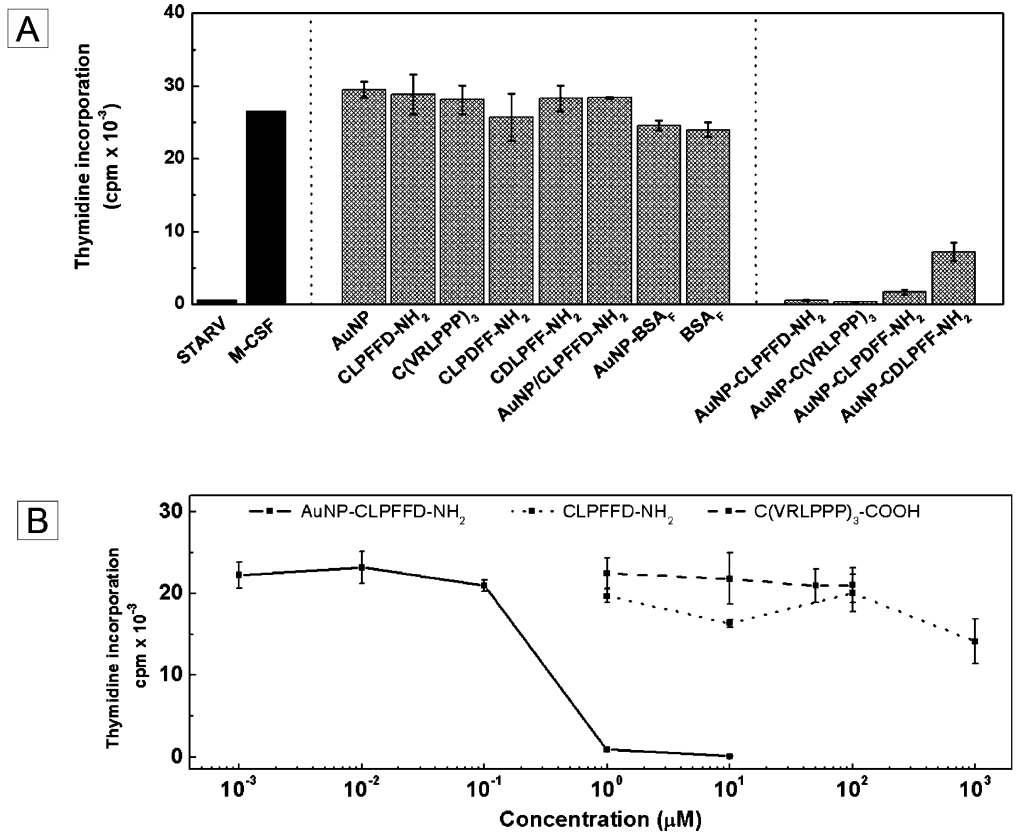

Figure 3. (A) Macrophage thymidine incorporation assays of Au NPs, peptides, and conjugates. Quiescent macrophages were stimulated with 1200 U/mL of M-CSF in the presence of the indicated substances. After 24 h, thymidine incorporation was measured and proliferation studies were performed as described in materials and methods. Similar results were found in all cases, the peptide-conjugated NPs inhibit the macrophage proliferation while the peptides or Au NPs do not. The simultaneous addition of Au NPs and CLPFFD-NH_2 (Au NPs/CLPFFD-NH_2) to the cell culture did not block macrophage proliferation suggesting that self-conjugation had not occurred. (B) Dose−response assays of Au NP-CLPFFD-NH_2 (AuNP−AGIP), CLPFFD-NH_2 (AGIP) and C(VRLPPP)$_3$ (AuNP−SAP). AuNP-CLPFFD-NH_2 inhibits macrophage proliferation in a dose-dependent manner while high doses of CLPFFD-NH_2 or C(VRLPPP)$_3$ failed to alter macrophage proliferation. Each experiment was performed in triplicate and results are expressed as the mean ± SD.

such as TNF-α, IL-β, and IL6 and the induction of nitric oxide synthase (NOS2) in order to signal invasion and eliminate the invaders.[21] The potential pro-inflammatory response of macrophages to Au NP conjugates, along with the necessary controls, was studied analyzing both cytokines production and macrophage proliferation.

Starved macrophages do not proliferate until the addition of their specific growth factor, the Macrophage Colony Stimulating Factor (M-CSF). DNA synthesis is then induced, which correlates with an increase in the number of cells. Macrophage proliferation was assessed by radioactive thymidine incorporation. Macrophages were exposed, after synchronization, to the indicated substance for 24 h as in previously described experiments.[22] To synchronize the macrophages they were rendered quiescent prior to any assay with an 18 h deprivation of M-CSF.

Macrophage proliferation in the presence of M-CSF was not affected by either citrate-stabilized Au NPs, AuNP-BSA_F or peptides even at concentrations over a thousand times higher, whereas the corresponding conjugates completely blocked proliferation (Figure 3A) in a dose dependent manner (Figure 3B). Moreover, this effect seems, to some extent, to be independent of peptide size, charge, and composition, but not on the coating order. CLPFFD-NH_2 ((AGIP), a short peptide of 6 amino acids) and C(VRLPPP)$_3$ ((SAP), a longer peptide of 19 amino acids) are chemically and structurally different and produce similar effects, since both have hydrophobic domains that help packing.[12] Similarly, CLPDFF-NH_2 (ISO1) and CDLPFF-NH_2 (ISO2) possess a different polarity and therefore a different degree of order, and produce a different degree of proliferation arrest.

It is remarkable that the simultaneous addition of Au NPs and CLPFFD-NH_2 (AGIP) to the cell culture did not block macrophage proliferation, suggesting that self-conjugation has not occurred because of medium proteins competing with CLPFFD-NH_2 (AGIP) for the NP surface.

To follow our studies the potential pro-inflammatory response of these cells to NP conjugates and controls was studied by analyzing the induction of cytokines. For the cytokines production assays, bacterial lipopolysaccharide (LPS), a major component of the outer mem-

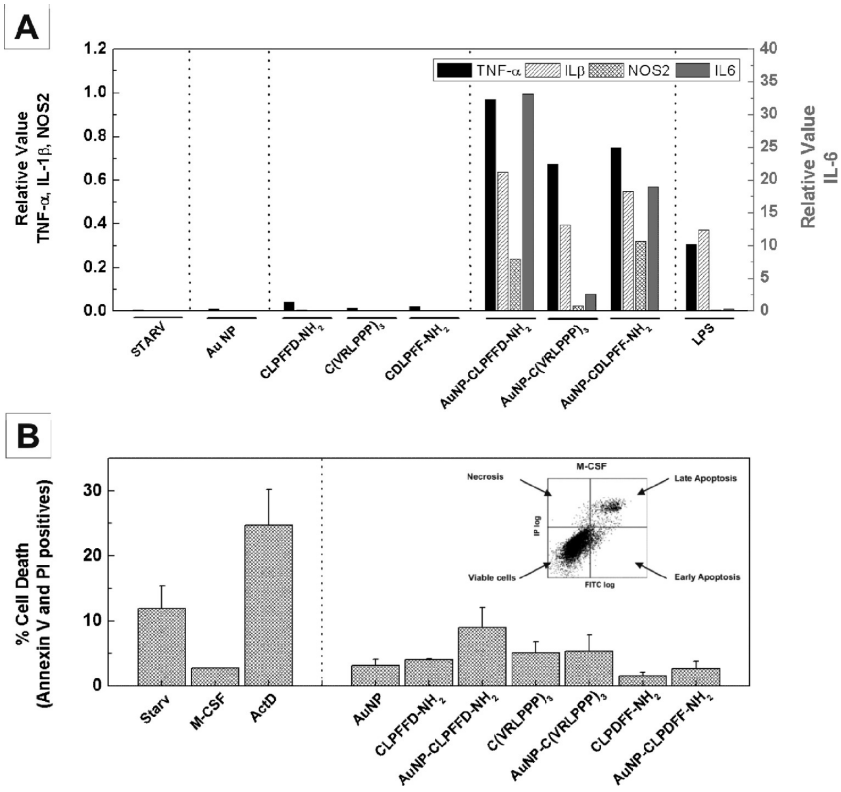

Figure 4. (A) Macrophage pro-inflammatory response toward Au NPs and their conjugates. Peptides conjugated to NPs induced a pro-inflammatory response in macrophages as can be measured by real time PCR. mRNA levels of TNF-α, IL-1β, IL-6, and NOS2 in relation to β-actin of macrophages stimulated for 6 h with LPS (10 ng/mL) or with the indicated substances (1 μM) in the presence of M-CSF. (B) Cell viability experiments. Neither peptides nor their conjugates affected cell viability. The cytotoxic effects of peptides and conjugates on macrophages incubated with M-CSF in the presence of the indicated substances during 24 h were assessed by Annexin V and propidium iodide determination. Actinomycin D (5 μg/mL) was used as a positive control of cell death. Each experiment was performed in triplicate and results are expressed as the mean ± SD. Inset plot presents representative FACS diagram of M-CSF control.

brane of Gram-negative bacteria, was used as a positive control at subsaturant concentration. Transcriptional induction of these molecules was analyzed *via* real-time PCR of extracted RNA under strict LPS-free conditions. According to the proliferation arrest, results show that neither peptides nor citrate-stabilized Au NPs activated any pro-inflammatory response since both the cytokines and NOS2 levels were similar to the untreated starved control (Figure 4A). However, an exacerbated cytokine and nitric oxide synthase induction was observed in the case of peptide-conjugated Au NPs, indicating a classical macrophage pro-inflammatory response toward pathogens. These observations are consistent with those where conjugates produced severe anaphylactic shocks in lab mice.

It is again notable that the particular type of response seemed to be dependent upon the peptide sequence, as it also happens in the presence of LPS from different bacterial species.[23,24] In the same way, although all studied conjugates induced the synthesis of TNF-α and IL-1β typically involved in fever, osteolysis, leucopenia, and hypotension, only AuNP-CLPFFD-NH_2 (AuNP−AGIP) was able to induce significant IL-6 production, which plays a role in inflammation mainly as an inducer of acute phase proteins.[25] Furthermore, NOS levels were insignificant in the presence of AuNP-$C(VRLPPP)_3$ (AuNP−SAP) conjugates. This data suggests that by modifying the nature of the peptide, the immune system can be modulated to promote different defense/inflammatory responses.

To verify that conjugate effects on macrophage biology were specific and not a reflection of compromised cell viability, necrosis and apoptosis assays were conducted by flow cytometry using Annexin V in combination with propidium iodide[22] (Figure 4B). Annexin V assay provides a simple and effective method to detect apoptosis at a very early stage. It takes advantage of the fact that phosphatidylserine (PS) is translocated from the inner (cytoplasmic) side of the plasma membrane to the outer (cell surface) side soon after the induction of apoptosis. PS on the outer side is able to bind annexin V, providing a simple staining assay. On the other hand, propidium iodide (PI), which monitors plasma membrane integrity, provides the detection of necrotic cells. ActinomycinD, a transcription inhibitor, was used as a positive control of apoptosis. In Figure 4B the percentage of cell death is the sum of positive measurements in both PI and Annexin V assays. None of the substances used in this study compromised cell viability, indicating that their effects on proliferation were specific. These data verify that it is possible to modify macrophage biology (activation of effectors functions), inducing a specific blockage of cell cycle progression, without causing nor altering cell viability, by the conjugation of different peptides to Au NPs.

Stopping proliferation and production of cytokines implies the engagement of phagocytosis. To investigate macrophage response and phagocytic activity in the presence of Au NP conjugates, we performed TEM studies. Macrophages were exposed to Au NPs and AuNP-CLDPFF-NH_2 (AuNP-C-AGIP) for different times: 15 and 30 min and 1, 2, 6, 12, and 24 h. As shown in Figure 5, an early internalization of the Au NP conjugates occurs at 30 min, with the maximum number of Au NPs inside the macrophages at 6 h and virtually none after 12 h. The rapid processing of Au NP conjugates seems to correlate with the observed pro-inflammatory response, thus preventing further internalization of Au NP conjugates. Incubating macrophages with nonconjugated Au NPs, or BSA-digest-coated Au NPs revealed no internalization at any time even after thorough TEM

observation. The data indicates that macrophages pro-inflammatory responses in the presence of peptide conjugates and the vesicle internalization of these conjugates are reminiscent of the typical pattern of some Toll-like receptor (TLR) mediated mechanisms. Since the main TLR involved in the pro-inflammatory production of TNF-α and IL-1β is TLR-4, we will study the role of this TLR in the effects of peptide conjugates on macrophages. TLR-4 deficient mice have a spontaneous mutation in the TLR-4 which leads to LPS resistance, therefore LPS will be our positive control and we will exclude the presence of endotoxin by testing macrophage proliferation in the presence of polymixin B. This antibiotic binds to the lipid portion of LPS and interferes the interaction with the TLR-4. As controls we will use mice from the same genetic background but with functional TLR-4.

In the recent years, a clear relationship between protein quaternary structure and higher order organization and immunogenicity has emerged.[26,27] Not surprisingly, many viruses exhibit a quasicrystalline, highly organized surface that displays a regular array of epitopes. Thus, the presentation of an antigen in a highly ordered and repetitive manner normally provokes strong antibody responses, whereas the same antigen presented as a monomer is nonimmunogenic.[5,28−30] Here special attention should be made to virus-like particles (VLPs) formed by certain viral proteins.[31,32] Virus-like particles consist of viral structural proteins that, when overexpressed, spontaneously self-assemble into particles that are antigenically indistinguishable from infectious viral or subviral particles. However, proteins that spontaneously assemble to highly repetitive structures are rare exceptions. In this sense, NPs have been recently used to electrostatically assist the assembly of brome mosaic virus proteins in preserving virus native size, structure, and physicochemical properties.[33] However, this electrostatic bonding needs an excess of conjugated protein in order to be stable and in equilibrium, and may loose stability *in vivo*.

In our case, we *force* the peptides to self-assemble on the Au surface *via* a cysteine and we use the peptide chain to control the degree of packing (and therefore the degree of immune response). Regarding CLPFF*D*-NH_2 (AGIP) and isomers, amino acids L, P, and F are hydrophobic and only the amino acid *D* presents a negative charge at physiological pH, while C is neutral. In this case the peptide adopts an extended conformation with the *D* residue placed away from the gold surface leading to a higher degree of packing.[13] On the other hand, when the *D* residue is near the Au NP surface (AuNP-*CD*LPFF-NH_2) (AuNP−ISO2), a higher repulsion between *D* residues and exposure of the hydrophobic residues, leads to a lower degree of packing. In the case of CLP*D*FF-NH_2 (ISO1) an intermediate situation occurs. These results were confirmed by circular dichroism (CD).[17] Thus, the degree of packing is AuNP-CLPFFD-NH_2 > AuNP-CLPDFF-NH_2 (ISO 1) > AuNP-CDLPFF-NH_2 (ISO 2). This is consistent with the observed degree of proliferation arrest (Figure 3A) and conjugate characterization. Similarly $(VRLPPP)_3$, with

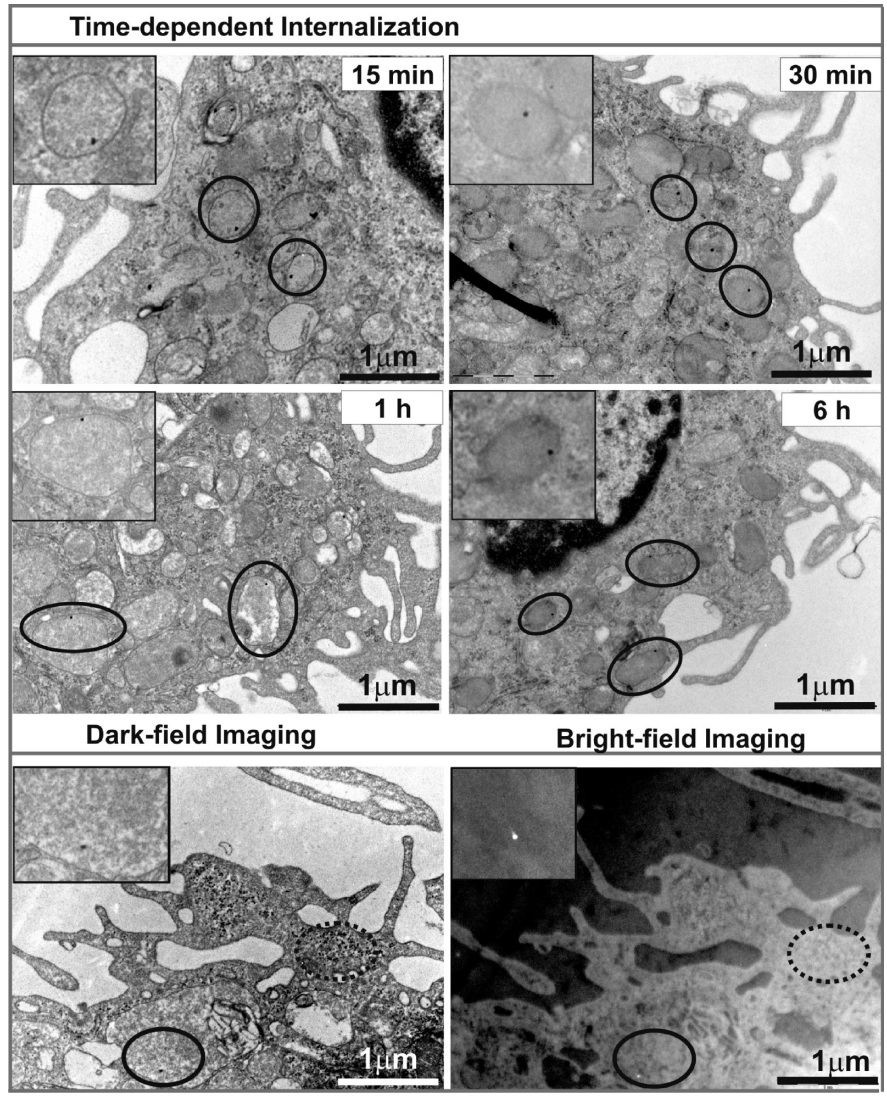

Figure 5. Internalization of Au NPs conjugates observed by transmission electron microscopy (TEM). (Top) Representative resin-tomography images revealing internalization of AuNP-CLPFFD-NH_2 (AuNP−AGIP) at 15 and 30 min and 1 and 6 h. (Bottom) Dark-field imaging and the high contrast of the Au NPs allowed us to easily distinguish the latter against ribosome and other high-contrast organelles. Scale bars are 1 μm.

aminoacid V and P being hydrophobic, yields highly packed layers, while the conjugation to BSA fragments (or cell media consisting in DMEM +10% FBS) produces disordered coating layers and no response from the macrophages. Thus, UV−vis and ζ-potential measurements are consistent with a higher degree of packing density in the strong immuno-activator AuNP-CLPFFD-NH_2 conjugate with respect to the weak immuno-activator AuNP-ISO2 conjugate, or to the non-imuno-activator AuNP-BSA_F conjugate. Thus, while the red-shift of the AuNP-CLPFFD-NH_2 (AuNP−AGIP) leads to a peak at 526 nm, in the case of AuNP-BSA_F it is 522 nm and in the case of the AuNP-ISO2 it is 524.5 nm. Similarly, while the drop of ζ-potential is large in the case of AuNP-CLPFFD-NH_2 (AuNP−AGIP), −7.3 mV, it is mild in the case of AuNP-BSA_F, −19,6 mV. All this underlying a correlation between coating density and macrophage activation.

Traditionally, it has been difficult to separate the role of epitope organization from the role of local epitope concentrations because highly organized epitopes are usually particulate whereas nonorganized epitopes are more soluble. To compare the effect of peptide aggregation we used $(VRLPPP)_3$ (SAP) peptide, which spontaneously aggregates at concentrations larger than 5 μM. In a dose dependent manner, macrophages were exposed to SAP concentrations up to 100 μM. It is known that at concentrations of 50 μM the peptide is already completely aggregated.[34] Aggregates of SAP peptide did not stop proliferation (Figure 3B), which means that they were unable to activate the immune system even at the employed high concentrations, while the conjugation of SAP peptide to Au NPs at 1 μM concentrations completely activated the immune system (Figure 3B), blocked the proliferation, and induced production of cytokines. Taking into account these results, it seems that the condition for the activation of macrophage response is related to the homogeneity of the coating layer. It is interesting to notice that particle size also plays an important role in the *in vivo* reticuloendothelial system activity. The universal trend is that the smaller particles have a substantially longer lifetime in the blood than the larger particles, in such a way that it was assumed that particles as small as 10 nm would not significantly activate the immune system.[35]

CONCLUSIONS

In light of the decreasing probability of natural infection, the acceptance of vaccine-induced side effects is continuously decreasing. Consequently, modern vaccines are usually produced recombinantly and do not replicate in the host. Unfortunately, isolated soluble components of viruses and other pathogens are often poorly immunogenic in the absence of nonspecific inflammatory stimuli.[36] Thus, tools to improve antigen presentation to the immune system based on inorganic nanoparticles and rational design may provide a useful toolkit for vaccinologists despite their small sizes (it was suggested that immune system evasion and long systemic circulation times by the particles are possible if they were of "ultra-low" size—usually <100 nm in diameter—and have surface hydrophilicity[35]). This may also serve to change and modulate immune response in the fight against allergies, rejection, cancer, and autoimmune diseases. This is also relevant for future developments of NP-based medical devices which have to travel to distant organs avoiding the immune system (and avoiding inflammation) before reaching their target. In addition two other aspects might be considered. In first place, conjugation protects against systemic degradation.[37,38] And second, NPs change biodistribution of their attached molecules[39] in such a way that they are accumulated in organs with high phagocytic activity like the liver, spleen, or the lymph nodes, the last being where the adaptive immune response is mainly produced.[40]

EXPERIMENTAL SECTION

Chemicals. All chemicals used were of highest available purity, and were supplied by Merck, Sigma-Aldrich, Fluka. The Millipore water had a resistance of 18.2 MΩ cm. Recombinant M-CSF (1200 U/mL ≅ 10 ng/mL) was obtained from R&D Systems Inc. (Minneapolis, MN), and alternatively, we used L-cell conditioned medium as the source of M-CSF. All reagents were prepared following the manufacturer's recommendations.

Techniques. UV−visible spectra were acquired with a Shimadzu UV-2400 spectrophotometer. Dynamic light scattering (DLS) measures were made with a Malvern ZetaSizer Nano ZS instrument operating at a light source wavelength of 532 nm and a fixed scattering angle of 173°. Zeta potential was determined using a Malvern ZetaSizer analyzer. These measurements were carried out using a control pH of 7.0. Transmission electron microscopy images were recorded with a JEOL 1010 microscope which operates at 80 kV. Real time-PCR was carried out with 2X SYBR Green PCR Master Mix using the ABI Prism 7900 detection system (Applied Biosystems, Foster City, CA).

Synthetic Procedures. Gold nanoparticles (Au NPs) were synthesized as following: a solution of sodium citrate 2.2 mM in Milli-Q water (150 mL) was heated to reflux with a heating mantel in a 250 mL three-necked round-bottom flask for 15 min under vigorous stirring. After boiling had commenced, 1 mL of HAuCl4 23.4 mM was injected. The resulting particles were stabilized with negatively charged citrate ions and were thus well suspended.

Peptide synthesis: CLPFFD (AGIP) was synthesized by solid-phase synthesis using the 9-fluorenylmethoxycarbonyl/tert-butyl (Fmoc/tBu) strategy and a Multiple Advanced Chemtech 496 Synthesizer. Rink amide resin, Nα-Fmoc-protected amino acids (4 equiv)/HBTU(4 equiv)/HOBt(4 equiv) and DIEA(8 equiv) were used. Fmoc protecting group was cleaved by treatment with a solution of 25% piperidine in DMF. Peptides were cleaved from the resin by treatment with 95% TFA, 2.5% TIS, 2.5% water for 2 h. $C(VRLPPP)_3$, (SAP) was synthesized manually by solid-phase synthesis using the 9-fluorenylmethoxycarbonyl/tert-butyl (Fmoc/tBu) strategy. 2-Chlorotrityl resin, Nα-Fmoc-protected amino acids (2 equiv)/TBTU(2 equiv) and DIEA(6 equiv)

were used. As a protecting group for the Arg side-chain, 2,2,4,6,7-pentamethyldihydrobenzofurane-5-sulfonyl (Pbf) was used. The Fmoc protecting group was cleaved by treatment with a solution of 20% piperidine in DMF (2 × 10 min). To incorporate the Fmoc-Arg(Pbf)-OH, the TBTU was replaced by PyBOP (2 equiv). C-SAP was cleaved from the resin by treatment with 95% TFA, 2.5% TIS, 2.5% water for 1 h 30 min. All peptides were purified by semi-preparative RP-HPLC and characterized by MALDI-TOF mass spectrometry.

Gold Nanoparticles Conjugation. An aqueous peptide solution (20 μM) was added to the Au NP solution and stirred for 30 min at room temperature. Excess peptides were removed from the NPs by dialysis (3500 or 6-8000 MWCO depending on the sequence, Spectrum Lab, Rancho Dominguez, CA) for 3 days at room temperature. BSA degradation and reduction: BSA (Cohn Fraction V, Fluka) was degraded with trypsin (trypsin from bovine pancreas, E.C. 3.4.21.4, Roche).

BSA was incubated at 37 °C dissolved in Tris · HCl 100 mM at 150 μM, and trypsin was added at the final concentration of 35.8 mg/mL (3.94 U/mL, U: Chromozym Try as a substrate). After 24 h at 37 °C, tris(2-carboxyethyl) phosphine hydrochloride (TCEP) obtained from Fluka at a final concentration of 10.5 mM was added and incubated during 1 h 30 min at room temperature to reduce disulfide bonds. This solution was conjugated to Au Np with the same protocol used for the different peptides.

Cell Culture. Primary cultures of bone-marrow-derived macrophages were obtained from BALB/c mice (Harlan Ibérica, Barcelona, Spain) and cultured as previously described during 6 days at 37 °C and 5% CO_2 incubators in DMEM (BioWhittaker-Cambrex, Emerainville, France), supplemented with 20% FCS and 30% L-cell conditioned media. The use of animals was approved by the Animal Research Committee of the University of Barcelona (No. 2523). To render macrophages quiescent, they were deprived of M-CSF for 18 h before stimulation.

Proliferation Assay. After 24 h of treatment, cells were pulsed with 3H-dThd (1 μCi/mL) (Amersham Pharmacia Biotech, Piscataway, NJ) for 6 h as previously described. After stimulation, cells were fixed with MeOH 70% at 4 °C overnight. Then, three washes of TCA 10% were performed and cells were lysed with NaOH plus SDS. 3H incorporation was mesured by standard liquid scintillation. Each point was performed in triplicate and the results were expressed as the mean ± SD.

Real-Time PCR. RNA Extraction and Real-Time PCR: Total RNA was extracted with the RNA Kit EZ-RNA (Biological Industries, Kibbutz beit hemeek, Israel) as indicated. cDNA was obtained from 1 μg of total RNA using M-MLV Reverse Transcriptase (Promega, Madison, WI) as described. Primer Express software (Applied Biosystems) was used to design primer sequences used for TNF-α, IL-1β, IL-6, and NOS2. Specific primer pairs were CCTTGTTGCCTCCTCTTTT GC and TCAGTGATGTAGCGACAGCCTG for TNF-α, CCTGTGTTTTCCTCCTTGCCT and GCCTAATGTCCCCTTGAATCAA for IL-1β, CAGAAGGAGTGGCTAAGGACCA and ACGCACT AGGTTTGCCGAGTAG for IL-6, GCCACCAACAATGGCAACA and GTACCGGATGAGCTGTG AATT for NOS2, ACTATTGGCAACGAGCGGTTC and AAGGAAGGCTGGAAAAGAGCC for β-actin, forward and reverse, respectively. Thermal cycling conditions were 94 °C, 30 s; 60 °C, 30 s; 72 °C, 30s for 35 cycles. Each sample was analyzed in triplicate. Expression levels were normalized to β-actin. Relative values from a representative experiment out of two independent experiments are shown.

TEM Preparation. Cells were fixed with a glutaraldehide 2.5% solution in PB 0.1 M for 1 h. After that cells were scraped, centrifuged at 4 °C, 2500 rpm, 10 min, and washed with PB 0.1 M. After the staining with OsO_4 1% for 1 h, cells were dehydrated in acetone at 4 °C and infiltered in Spurr epoxy resin. After embedment (60 °C, 48 h), 50 nm ultrathin sections were created with an ultramicrothom. Finally cells were stained with uranyl acetate and lead citrate.

Acknowledgment. This work was supported by Grants MEC-FEDER (BIO2005-00295 and NAN2004-09159-C04-02 to E.G., BFU2004-05725/BMC and BFU2007-63712/BMC to A.C., SAF2006-26676-E to J.L., and INGENIO 2010 NANOBIOMED and MAT2006-13572-C02-02 to V.P.).

Supporting Information Available: Materials and methods, conjugates characterization (including gel electrophoresis), cell flow cytometry, and exclusion of LPS contamination. This material is available free of charge *via* the Internet at http://pubs.acs.org.

REFERENCES AND NOTES

1. Alivisatos, A. P. Less Is More in Medicine. *Sci. Am.* **2001**, *285*, 66–73.
2. Turvey, S. E.; Hawn, T. R. Towards subtlety: Understanding the Role of Toll-like Receptor Signaling in Susceptibility to Human Infections. *Clin. Immunol.* **2006**, *120*, 1–9.
3. Krieg, A. M. Therapeutic Potential of Toll-like Receptor 9 Activation. *Nat. Rev. Drug Discovery* **2006**, *5*, 471–484.
4. Beutler, B. Tlr4: Central Component of the Sole Mammalian LPS Sensor. *Curr. Opin. Immunol.* **2000**, *12*, 20–26.
5. Bachmann, M. F.; Rohrer, U. H.; Kundig, T. M.; Burki, K.; Hengartner, H.; Zinkernagel, R. M. The Influence of Antigen Organization on B Cell Responsiveness. *Science* **1993**, *262*, 1448–1451.
6. Spohn, R.; Buwitt-Beckmann, U.; Brock, R.; Jung, G.; Ulmer, A. J.; Wiesmüller, K.-H. Synthetic Lipopeptide Adjuvants and Toll-like Receptor 2—Structure−Activity Relationships. *Vaccine* **2004**, *22*, 2494–2499.
7. Pfaller, T.; Puntes, V.; Casals, E.; Duschl, A.; Oostingh, G. J. *In Vitro* Investigation of Immunomodulatory Effects Caused by Engineered Inorganic Nanoparticles—The Impact of Experimental Design and Cell Choice. *Nanotoxicology* **2009**, *99999*, 1–14.
8. Lucarelli, M.; Gatti, A. M.; Savarino, G.; Quattroni, P.; Martinelli, L.; Monari, E.; Boraschi, D. Innate Defence Functions of Macrophages Can Be Biased by Nano-Sized Ceramic and Metallic Particles. *Eur. Cytokine Network* **2004**, *15*, 339–346.
9. Kogan, M. J.; Bastus, N. G.; Amigo, R.; Grillo-Bosch, D.; Araya, E.; Turiel, A.; Labarta, A.; Giralt, E.; Puntes, V. F. Nanoparticle-Mediated Local and Remote Manipulation of Protein Aggregation. *Nano Lett* **2006**, *6*, 110–115.
10. Fernandez-Carneado, J.; Kogan, M. J.; Castel, S.; Giralt, E. Potential Peptide Carriers: Amphipathic Proline-Rich Peptides Derived from the N-Terminal Domain of Gamma-Zein. *Angew. Chem., Int. Ed.* **2004**, *43*, 1811–1814.
11. Sellers, H.; Ulman, A.; Shnidman, Y.; Eilers, J. E. Structure and Binding of Alkanethiolates on Gold and Silver Surfaces: Implications for Self-Assembled Monolayers. *J. Am. Chem. Soc.* **1993**, *115*, 9389–9401.
12. Zhu, T.; Vasilev, K.; Kreiter, M.; Mittler, S.; Knoll, W. Surface Modification of Citrate-Reduced Colloidal Gold Nanoparticles with 2-Mercaptosuccinic Acid. *Langmuir* **2003**, *19*, 9518–9525.
13. Pale-Grosdemange, C.; Simon, E. S.; Prime, K. L.; Whitesides, G. M. Formation of Self-Assembled Monolayers by Chemisorption of Derivatives of Oligo(ethylene glycol) of Structure $HS(CH_2)_{11}(OCH_2CH_2)$ *m*OH on gold. *J. Am. Chem. Soc.* **1991**, *113*, 12–20.
14. Bensebaa, F.; Zhou, Y.; Deslandes, Y.; Kruus, E.; Ellis, T. H. XPS Study of Metal-Sulfur Bonds in Metal-Alkanethiolate Materials. *Surf. Sci.* **1998**, *405*, L472−L476.
15. Pujals, S.; Bastús, N. G.; Pereiro, E.; López-Iglesias, C.; Puntes, V. F.; Kogan, M. J.; Giralt, E., Shuttling Gold Nanoparticles into Tumoral Cells with an Amphipathic Pro-rich Peptide. ChemBioChem, in press.
16. Zanchet, D.; Micheel, C. M.; Parak, W. J.; Gerion, D.; Alivisatos, A. P. Electrophoretic Isolation of Discrete Au Nanocrystal/DNA Conjugates. *Nano Lett.* **2001**, *1*, 32–35.
17. Olmedo, I.; Araya, E.; Sanz, F.; Medina, E.; Arbiol, J.; Toledo, P.; Alvarez-Lueje, A.; Giralt, E.; Kogan, M. J. How Changes in the Sequence of the Peptide CLPFFD-NH2 Can Modify the Conjugation and Stability of Gold Nanoparticles and Their Affinity for β-Amyloid Fibrils. *Bioconjugate Chem.* **2008**, *19*, 1154–1163.
18. Celada, A.; Gray, P. W.; Rinderknecht, E.; Schreiber, R. D. Evidence for a Gamma-Interferon Receptor That Regulates Macrophage Tumoricidal Activity. *J. Exp. Med.* **1984**, *160*, 55–74.

19. Vadiveloo, P. K. Macrophages—Proliferation, Activation, And Cell Cycle Proteins. *J. Leukocyte Biol.* **1999**, *66*, 579–582.
20. Xaus, J.; Comalada, M.; Valledor, A. F.; Cardo, M.; Herrero, C.; Soler, C.; Lloberas, J.; Celada, A. Molecular Mechanisms Involved in Macrophage Survival, Proliferation, Activation or Apoptosis. *Immunobiology* **2001**, *204*, 543–50.
21. Valledor, A. F.; Xaus, J.; Marques, L.; Celada, A. Macrophage Colony-Stimulating Factor Induces the Expression of Mitogen-Activated Protein Kinase Phosphatase-1 through a Protein Kinase C-Dependent Pathway. *J. Immunol.* **1999**, *163*, 2452–2462.
22. Sanchez-Tillo, E.; Comalada, M.; Xaus, J.; Farrera, C.; Valledor, A. F.; Caelles, C.; Lloberas, J.; Celada, A. JNK1 is Required for the Induction of Mkp1 Expression in Macrophages during Proliferation and Lipopolysaccharide-Dependent Activation. *J. Biol. Chem.* **2007**, *282*, 12566–12573.
23. Blondiau, C.; Lagadec, P.; Lejeune, P.; Onier, N.; Cavaillon, J. M.; Jeannin, J. F. Correlation between the Capacity to Activate Macrophages *in-Vitro* and the Antitumor-Activity *in-Vivo* of Lipopolysaccharides from Different Bacterial Species. *Immunobiology* **1994**, *190*, 243–254.
24. Zhan, Y. F.; Cheers, C. Differential Induction of Macrophage-Derived Cytokines by Live and Dead Intracellular Bacteria *in-Vitro*. *Infect. Immun.* **1995**, *63*, 720–723.
25. Cavaillon, J. M. Interleukins and Inflammation. *Pathol. Biol.* **1990**, *38*, 36–42.
26. Salk, D.; Van Wezel, A.; Salk, J. Induction of Long-Term Immunity to Paralytic Poliomyelitis by Use of Non-infectious Vaccine. *The Lancet* **1984**, *324*, 1317–1321.
27. Sabin, A. B. Oral Poliovirus Vaccine: History of Its Development and Use and Current Challenge to Eliminate Poliomyelitis from the World. *J. Infect. Dis.* **1985**, *151*, 420–436.
28. Bachmann, M. F.; Zinkernagel, R. M. The Influence of Virus Structure on Antibody Responses and Virus Serotype Formation. *Immunol. Today* **1996**, *17*, 553–558.
29. Feldmann, M.; Basten, A. The Relationship between Antigenic Structure and the Requirement for Thymus-Derived Cells in the Immune Response. *J. Exp. Med.* **1971**, *134*, 103–119.
30. Jegerlehner, A.; Storni, T.; Lipowsky, G.; Schmid, M.; Pumpens, P.; Bachmann, M. Regulation of IgG Antibody Responses by Epitope Density and CD21-Mediated Costimulation. *Eur. J. Immunol.* **2002**, *32*, 3305–3314.
31. Noad, R.; Roy, P. Virus-like Particles As Immunogens. *Trends Microbiol.* **2003**, *11*, 438–444.
32. Johnson, J. E.; Chiu, W. Structures of Virus and Virus-like Particles. *Curr. Opin. Struct. Biol.* **2000**, *10*, 229–235.
33. Chen, C.; Daniel, M. C.; Quinkert, Z. T.; De, M.; Stein, B.; Bowman, V. D.; Chipman, P. R.; Rotello, V. M.; Kao, C. C.; Dragnea, B. Nanoparticle-Templated Assembly of Viral Protein Cages. *Nano Lett.* **2006**, *6*, 611–615.
34. Pujals, S.; Fernandez-Carneado, J.; Lopez-Iglesias, C.; Kogan, M. J.; Giralt, E. Mechanistic Aspects of CPP-Mediated Intracellular Drug Delivery: Relevance of CPP Self-Assembly. *Biochim. Biophys. Acta, Biomembr.* **2006**, *1758*, 264–279.
35. Podsiadlo, P.; Sinani, V. A.; Bahng, J. H.; Kam, N. W. S.; Lee, J.; Kotov, N. A. Gold Nanoparticles Enhance the Anti-leukemia Action of a 6-Mercaptopurine Chemotherapeutic Agent. *Langmuir* **2008**, *24*, 568–574.
36. Bachmann, M. F.; Zinkernagel, R. M.; Oxenius, A. Cutting Edge Commentary: Immune Responses in the Absence of Costimulation: Viruses Know the Trick. *J. Immunol.* **1998**, *161*, 5791–5794.
37. Janes, K. A.; Calvo, P.; Alonso, M. J. Polysaccharide Colloidal Particles As Delivery Systems for Macromolecules. *Adv. Drug Delivery Rev.* **2001**, *47*, 83–97.
38. Chavany, C.; Saison-Behmoaras, T.; Doan, T. L.; Puisieux, F.; Couvreur, P.; Hélène, C. Adsorption of Oligonucleotides onto Polyisohexylcyanoacrylate Nanoparticles Protects Them Against Nucleases and Increases Their Cellular Uptake. *Pharm. Res.* **1994**, *11*, 1370–1378.
39. Casals, E.; Vázquez-Campos, S.; Bastús, N. G.; Puntes, V. Distribution and Potential Toxicity of Engineered Inorganic Nanoparticles and Carbon Nanostructures in Biological Systems. *TrAC Trends Anal. Chem.* **2008**, *27*, 672–683.
40. Wolfrum, C.; Shi, S.; Jayaprakash, K. N.; Jayaraman, M.; Wang, G.; Pandey, R. K.; Rajeev, K. G.; Nakayama, T.; Charrise, K.; Ndungo, E. M.; Zimmermann, T.; Koteliansky, V.; Manoharan, M.; Stoffel, M. Mechanisms and Optimization of *in Vivo* Delivery of Lipophilic siRNAs. *Nat. Biotechnol.* **2007**, *25*, 1149–1157.